Stem Cell Reports, Volume *12*

Supplemental Information

Neural Stem Cells of Parkinson's Disease Patients Exhibit Aberrant Mitochondrial Morphology and Functionality

Jonas Walter, Silvia Bolognin, Paul M.A. Antony, Sarah L. Nickels, Suresh K. Poovathingal, Luis Salamanca, Stefano Magni, Rita Perfeito, Fredrik Hoel, Xiaobing Qing, Javier Jarazo, Jonathan Arias-Fuenzalida, Tomasz Ignac, Anna S. Monzel, Laura Gonzalez-Cano, Luis Pereira de Almeida, Alexander Skupin, Karl J. Tronstad, and Jens C. Schwamborn

Supplemental Information

Neural stem cells of Parkinson's disease patients exhibit aberrant mitochondrial morphology and functionality

Jonas Walter[1,9], Silvia Bolognin[1,9], Paul M.A. Antony[1,7], Sarah L. Nickels[1,2,7], Suresh K. Poovathingal[1,7,#], Luis Salamanca[1], Stefano Magni[1], Rita Perfeito[3], Fredrik Hoel[4], Xiaobing Qing[1], Javier Jarazo[1], Jonathan Arias-Fuenzalida[1], Tomasz Ignac[1], Anna S. Monzel[1], Laura Gonzalez-Cano[1], Luis Pereira de Almeida[3,5], Alexander Skupin[1,6], Karl J. Tronstad[4], Jens C. Schwamborn[1,8*]

[1] Luxembourg Centre for Systems Biomedicine (LCSB), University of Luxembourg, L-4362 Belvaux, Luxembourg
[2] Life Science Research Unit (LSRU), University of Luxembourg, L-4362 Belvaux, Luxembourg
[3] CNC-Center for Neuroscience and Cell Biology, University of Coimbra, Rua Larga, Coimbra 3004-504, Portugal
[4] Department of Biomedicine, University of Bergen, 5020 Bergen, Norway
[5] Faculty of Pharmacy, University of Coimbra, Coimbra 3000-548, Portugal
[6] Center for Research of Biological Systems, University of California San Diego, La Jolla, CA 92093, USA
[7] These authors contributed equally to this work.
[8] Lead contact
[9] Equal first author contribution
[#] Current address: Single Cell Analytics & Microfluidics Core, VIB-KU Leuven, Herestraat 49, 3000 Leuven, Belgium
* Correspondence: jens.schwamborn@uni.lu (J.C.S.)

Supplemental Figures and Legends

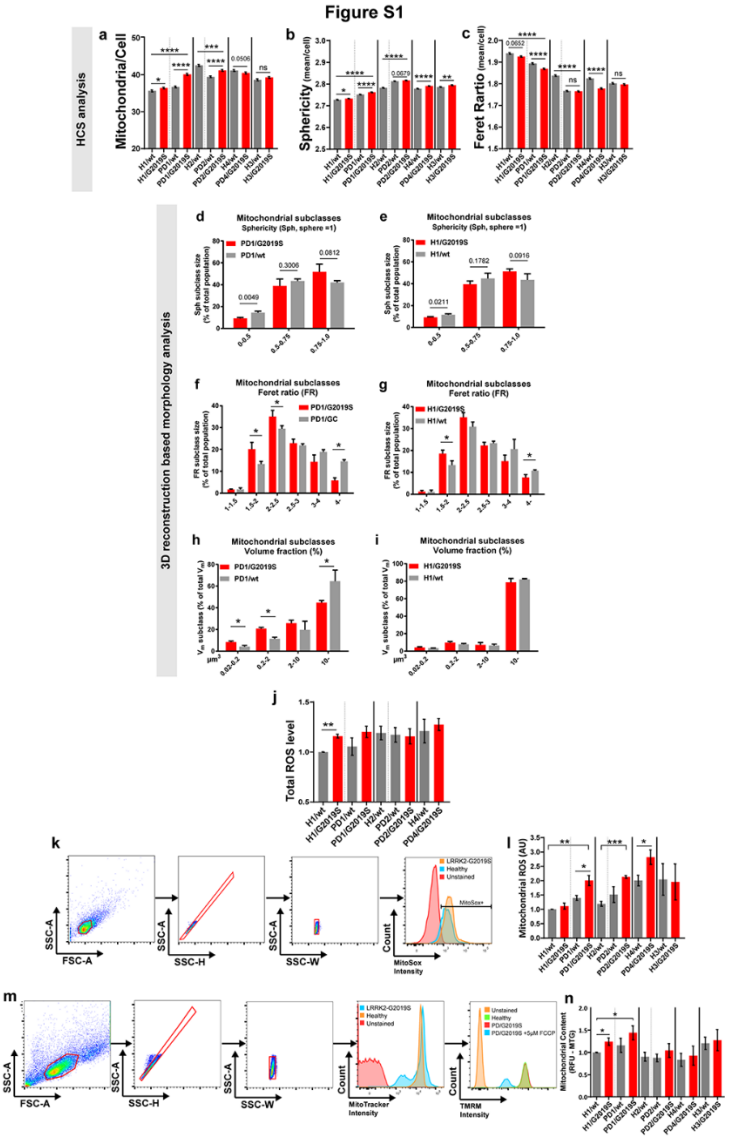

Figure S1. LRRK2-G2019S induces mitochondrial morphological alterations in NESC. Related to Figure 2.

(a-c) Graphs showing HCS-based mitochondrial morphometric analyses before the pooling described in **Figures 1a-c**. Statistical significance was assessed with Mann-Whitney test, N=3, n=3. **(d-i)** 3D mitochondrial morphology analysis (**Figures 1e-j**) in more detailed subclass comparison of: **(d-e)** mitochondrial volume; **(f-g)** Feret ratio; **(h-i)** mitochondrial sphericity, always comparing PD1 and H1 separately. Statistical significance tested via Student's t-test, N=3, n=3. **(j)** Total ROS levels before the described pooling (**Figure 2k**), data normalized to H1, statistical significance tested via Student's t-test, N=5-6, n=3. **(k)** Example gating of flow cytometric of MitoSox (mitochondrial ROS) analysis (**Figures 1l, S1l**) showing all the gating combinations used, and the sample distribution in comparison to unstained control. **(l)** Mitochondrial ROS levels before the described pooling (**Figure 2l**), data normalized to H1, statistical significance tested via Student's t-test, N=4, n=1. **(m)** Example gating of flow cytometry MitoTracker/TMRM analysis showing all the gating combinations used, and the sample distribution in comparison to unstained control. **(n)** Graphs of mitochondrial content analysis using MitoTracker 488 relative fluorescence (RFU), data normalized to H1, significances tested via Student's t-test, N=4, n=2. For all panels, the data are presented as the mean ± SEM. N indicates the number of experimental repetitions, n indicates the number of technical replicates per cell line.

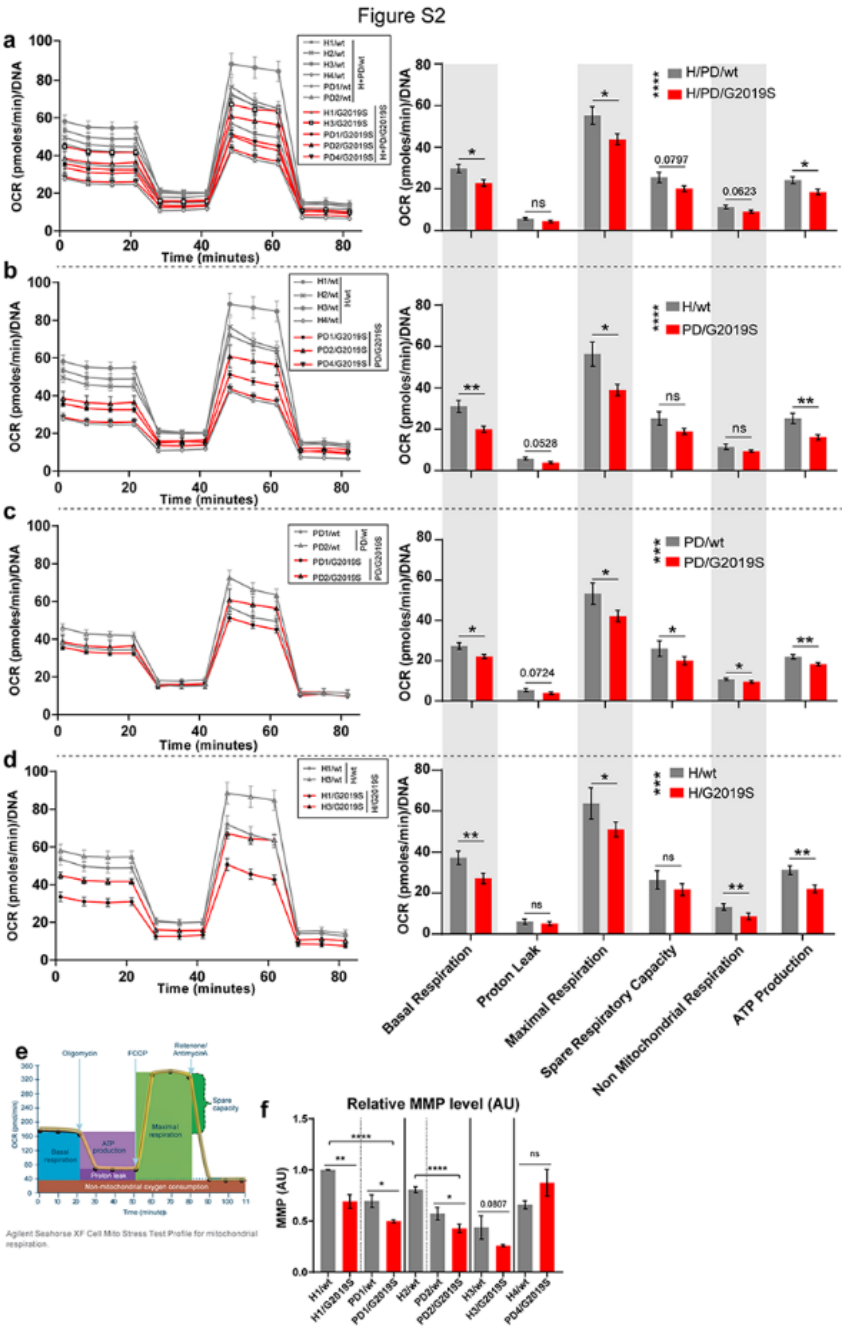

Figure S2. LRRK2-G2019S alters the oxygen consumption rate in NESCs. Related to Figure 3.

(a-d) Graphs showing OCR before the pooling described in **Figure 2a-d**. The OCR graphs on the left show the oxygen consumption over time. The bar graphs on the right visualize the data corresponding to the grouped time points per each feature assessed. Significance was tested via Student's t-test. 2-way ANOVA analysis was also performed and the significance is indicated in the bar-graph legends, N=3, n=8. **(e)** Manufacturer's OCR-graph, explaining the calculations underlying the relative respiratory capacity features. **(f)** Graphs showing the mitochondrial membrane potential (MMP) before the pooling in **Figure 3e**. Data was normalized to H1. Significance was tested via Student's t-test, N=4, n=2. For all panels, the data are presented as mean ± SEM. N indicates the number of experimental repetitions, n indicates the number of technical replicates per cell line.

Figure S3

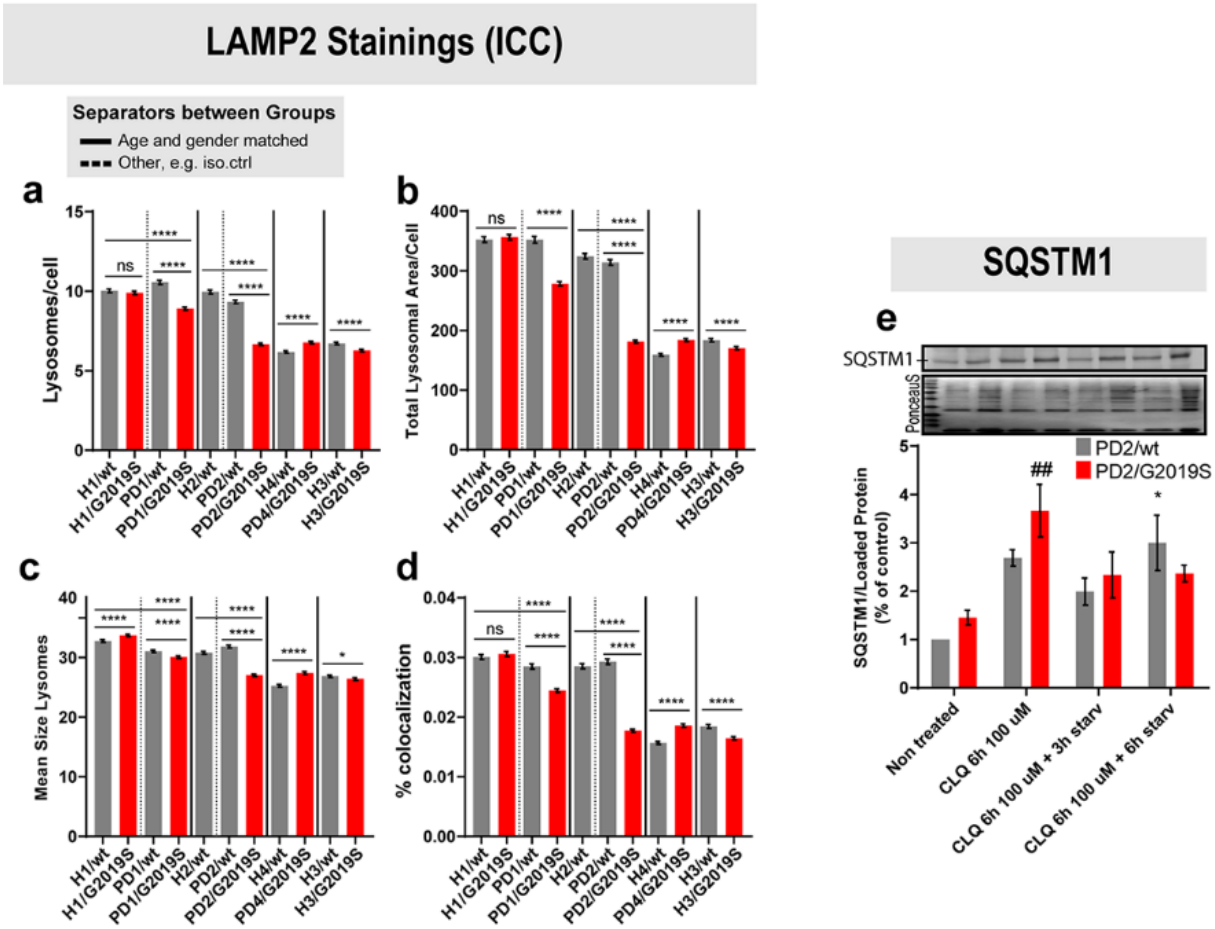

Figure S3. LRRK2-G2019S alters mitochondrial quality control in NESCs. Related to Figure 4.
(a-c) Bar graphs showing HCS analysis of the different cell groupings. **(a)** LAMP-2 puncta per cell, **(b)** total lysosomal area per cell, and **(c)** mean size lysosomes per cell (**Figures 4c-d**). Statistical significance was tested via Mann-Whitney test, N=3, n=3. **(d)** Graph showing the co-localization of LAMP-2 and TOM20 puncta per cell resulting from the HCS analysis, before the described pooling. Statistical significance was tested via Mann-Whitney test, N=3, n=3. **(e)** SQSTM1 level analysis shown for all conditions during the induction of autophagy via starvation, N=3, n=3. Statistical significance as determined by 2-way ANOVA and Tukey multiple comparisons test is indicated [* (comparison with untreated PD2.GC cells); ## (comparison with untreated PD2.G2019S cells)]. For all panels, the data are presented as mean ± SEM. N indicates the number of experimental repetitions, n indicates the number of technical replicates per cell line.

Table S1. Mitochondrial gene defined by the MitoCarta2.0.

Table S2. Differentially expressed genes identified when comparing LRRK2-WT and LRRK2-G2019S.

Supplemental Experimental Procedures

Cell Culture

iPSCs were maintained in E8 medium, on GelTrex matrix. Culture splits were performed using Accutase followed by overnight (o/n) incubation with 5 μM Y-27632 (Merck Millipore). NESCs were derived from iPSC as previously described (Reinhardt et al., 2013). Cells were maintained on MatriGel matrix NUNCLON plates. N2B27 maintenance media was used: Neurobasal, DMEM-F12 (1:1), 1x P/S, 1x L-Glutamine, B27 (1:100), N2 (1:200) (ThermoFisher) freshly supplemented with 3 μM CHIR(-99021) (Axon Medchem), 0.75 μM Purmorphamine (PMA) (Enzo Life Science) and 150 μM ascorbic acid (AA) (Sigma). Cells were seeded at $5*10^4$ cells/cm^2 (counted in a Countess II, AMQAX1000 ThermoFisher). For dopaminergic neuronal differentiation, NESCs were seeded at $5*10^4$ cells/cm^2 density either on MatriGel matrix coated NUNCLON or Cell Carrier-96 plates from Perkin Elmer for HCS analyses. Dopaminergic differentiation was initiated two days after initial cell seeding by the addition of differentiation media consisting of N2B27 freshly supplemented with: 10 ng/ml hBDNF (Peprotech), 10 ng/ml hGDNF (Peprotech), 500 μM dbcAMP (Peprotech), 200 μM ascorbic acid (Sigma), 1 ng/ml TGF-β3 (Peprotech), and 1 μM PMA (Enzo Life Science). PMA was withdrawn from the media after six days.

NGS preparation for Dropseq libraries

The 3' end enriched cDNA libraries were prepared by the tagmentation reaction of 600 pg cDNA library using the standard Nextera XT tagmentation kit (Illumina). The reactions were performed according to the manufacturer's instruction, except for the following two 400 nM primer sets (used instead of the kit provided primers): Primer 1 (AATGATACGGCGACCACCGAGATCTACACGCCTGTCCGCGGAAGCAGTGGTA TCAACGCAGAG T*A*C) and Primer 2 (N703: CAAGCAGAAGACGGCATACGAGATTTCTGC CTGTCTCGTGGGCTCGG for the PD2/G2019S samples and N709: CAAGCAGAAGACGGCATAC GAGATAGCGTAGCGTCTCGTGGGCTCGG for PD2/wt samples). The cycling program used for these samples was: 95°C for 30 s; fourteen cycles of 95°C for 10 s, 55°C for 30 s, 72°C for 30 s followed by a final extension step of 7°C for 5 min.Post PCR amplification, libraries were purified twice to reduce the primers and short DNA fragments, with 0.6x Agencourt AMPure XP beads (Beckman Coulter) followed by 1x Agencourt AMPure XP beads, in accordance with the manufacturer's protocol. Finally, the purified libraries were eluted in 15 μl of molecular grade water. Quality and quantity of tagmented cDNA library were evaluated using BioAnalyzer High Sensitivity DNA Chip. The average size of the tagmented libraries prior to sequencing was between 400-700.Purified Dropseq cDNA libraries were sequenced using an Illumina NextSeq 500 with the recommended sequencing protocol with the exception that 6 pM of custom primer (GCCTGTCCGCGGAAGCAGTGGTATCAACGCAGAGTAC) was used for priming of read 1. Further, paired-end sequencing was performed with reading 1 of 20 bases (covering the random cell barcode 1-12 bases and the rest 13-20 bases of the random molecular identifier, UMI) and read 2: 50 bases of the corresponding gene sequence.

Bioinformatics Processing of Dropseq data

FASTQ files were assembled from the raw BCL files using Illumina's bcl2fastq converter. FASTQ files were subsequently run through the FASTQC codes (Babraham bioinformatics; https://www.bioinformatics.babraham.ac.uk/projects/fastqc/) to check for the consistency in library qualities. The following parameters were evaluated for quality assessment: a) per base sequence quality (especially for read 2 of the gene related sequence); b) per base N content; c) per base sequence content and d) over-represented sequences. The libraries, which showed significant deviation, were re-sequenced. The FASTQ files were then merged and converted to binaries using PICARD's fastqtosam algorithm. Using the Dropseq bioinformatics pipeline, the sequencing reads were converted to digital gene expression matrix (DGE). The parameters used for the bioinformatics processing were consistent with the original Dropseq work (Macosko et al., 2015). To normalize the cells (equalize the transcript loading between the beads), the averaged normalized expression levels, $\log_2(TPM+1)$, was calculated. In accordance with the original Dropseq pipeline, to distinguish between the beads exposed to the cell and the beads which were blank, a cumulative function of the total number of transcripts per barcode was plotted. Then, a thresholding was performed on the resulting "knee plot" to estimate the beads exposed to the cell content. To filter the poor quality reads and cells reporting low transcript content, the following thresholds were used: only cells which expressed at least 1500 genes, and only genes expressed in at least 20 cells were considered for further analysis. The estimation of the highly variable genes and principal component analysis and tSNE dimensionality reduction was implemented

using SEURAT R package (http://satijalab.org/seurat/). The FASQT files have the GEO accession number GSE128040.

Analysis of Mitocondrial genes expression at the single cell level

Bioinformatics processing of the DropSeq data resulted in 8 gene expression matrices, one for each of the isogenic NESC pair (PD2/wt & PD2/G2019S) per time point extracted. Columns of these gene expression matrices represent individual cells, lines represent genes, and the entries represent the number of mRNA transcripts measured. The subsequent custom analysis pipeline was developed and implemented using Python programming language (version 3.6.0, with anaconda version 4.3.1). Since there was not a full overlap in genes of the resulting matrices, we first created for both genotypes at each time point a common list of expressed genes, which enabled us to analyze the pooled data of the NESC pair per time point. Moreover, in order to select only the highest quality data, we sorted the cells by the cumulative expression of all remaining genes. Only a subset of cells with the highest cumulative gene expression was considered for the analysis. In particular, only the 250 cells with the highest overall expression levels for each group (PD2/wt & PD2/G2019S) and each day were considered. The intention of this filtering step of all gene expression matrices was to attenuate the effect of noise originating from the acquisition process. It is worth mentioning that this conservative reduction to 2000 cells was more stringent than typical filtering in scRNA-seq quality control. Additionally, we normalized the gene expression matrix, for each particular group and day, by obtaining the standard score for each gene, i.e., we subtracted and divided the gene raw score of each cell respectively by the mean and the standard deviation of its row (gene).
To extract the relevant information on mitochondria, we defined a list of 1158 genes (**TABLE S1**) specific of mitochondria, based on MitoCarta2.0. We thus compared the expression of the corresponding genes between genotypes within sampling points. Since the gene expression levels are measured at the single cell level, instead of simply comparing the mean expression for all cells of each group, we analyzed the distribution of gene expression across cells. **Fig. 1c** histograms show the cumulative gene expression distributions for cells of each group and for each time point (columns). We defined cumulative gene expression as the sum of all mRNAs of the genes in the above mentioned list leading to a single cumulative score for each cell. Since the total numbers of mRNAs are not comparable between days, the values in the horizontal axis are normalized, separately for each day and each list of genes, to the maximum of the cumulative gene expression (across the genotypes PD2/wt & PD2/G2019S) for that particular time point. Thus, 1 corresponds to the maximal cumulative gene expression within one day, while 0 corresponds to no expression for each of the genes on the above mentioned list (**TABLE S1**), on that time point. Application of a z-test (corrected to allow the comparison of distributions with unequal variance) allowed assessing which individual panels present a statistically significant difference between the means of the cumulative gene expression of the genotypes. The test was corrected by including Bonferroni.

Analysis of differentially expressed genes (DEGs) in the single-cell RNA-Seq data

For each time point of the experiment, we determined how many genes were differentially expressed between LRRK2-WT and LRRK2-G2019S, by applying to all genes (independently for each gene) the following three statistical tests: a one-way ANOVA test, a one-way ANOVA test on ranks (Kruskal-Wallis test), and a test based on Mutual Information. The minimum p-value obtained by each gene across these three tests was retained, and any gene was considered differentially expressed with statistical significance when the corresponding p-value was below a threshold of 0.01.
In order to account for multiple testing, the Bonferroni correction was applied. The test was applied to all the approximately 20000 genes for each time point. The individual p-value for each gene is required to be $< 0.01/20000$ in order to claim statistical significance with an overall p-value < 0.01. We then computed the number of genes that were differentially expressed between genotypes with a statistical significance corresponding to a p-value < 0.01, for each day. In the results section, we also report the percentages, indicating how many of the mitochondrial specific genes are differentially expressed at each time point.

Immunocytochemistry

Cells were fixed using 4% paraformaldehyde (PFA) in 1x phosphosaline buffer (1xPBS), pH 7.4, for 15min at room temperature (RT). Unspecific antibody (AB) binding was avoided by blocking buffer incubation (5% FCS, 0.1%Tween20 in 1xTBST) for 1h at RT. Primary AB binding was performed for 48h at 4°C using indicated primary AB in blocking buffer. Three washing steps with 1xPBS were performed and the secondary ABs were incubated for

1h at RT (1:1000 dilution, including 1:1000 Hoechst33342). Following incubation, cells were washed 3x using 1xPBS. The following first antibodies were used: LAMP2 (DSHB, H4B4), and TOM20 (SantaCruz sc-11415).

2D Image analysis

Images were acquired sequentially on an Opera QEHS using a 60x (N.A. = 1.2) water immersion objective. Hoechst was excited at 405 nm laser and detected behind a 450/50 bandpass filter. Tom20_Alexa488 antibody was excited at 488 nm and detected behind a 520/35 bandpass filter. Lamp2_Alexa647 was excited at 640 nm and detected behind a 690/70 bandpass filter. Image analysis was implemented in Matlab (Mathworks). The Hoechst channel was low pass filtered, thresholded (>100), and connected components with less than 500 pixels were removed (NucleiMask1). Nuclei were split using a Laplacian of Gaussians of size 30 and standard deviation 10, thresholded (>0.12), and components with less than 2000 pixels were removed (NucleiContourMask). To refine the NucleiMask, the NucleiContourMask and resulting connected components with less than 2500 pixels were removed (NucleiMask2). Splitting was refined via Euclidean distance transform and watershed. Objects with less than 2500 pixels were removed (NucleiMask3). Cells were detected using low pass filtering of the phalloidin channel, thresholding (>20), and removal of connected components with less than 15000 pixels (CellMask). Single cell segmentation was based on Euclidean distance transform of NucleiMask3. Cells touching the image border were removed (CellStencil). For quality check, big objects (> 100000 pixels, NucleiMask4), as well as low sphericity objects were removed (NucleiMask5). The zones of the CellStencil passing this quality check were retained for further processing (CellStencilRefined). Mitochondria were segmented based on local image contrast as described previously (MitoMask), (Foster et al., 2016). Mitochondrial bodies were defined using image erosion of MitoMask with a sphere-shaped structuring element of radius 1. The mitochondrial surface was defined by subtracting the mitochondrial bodies from MitoMask (MitoSurfMask). Lysosomes were segmented based on the Lamp2 channel using a combination of local and global thresholding. For global thresholding, the raw channel was low pass filtered and thresholded (>75, LysoGlobalMask). For local thresholding, a difference of Gaussians was applied to the raw Lamp2 channel. The Foreground image was convolved with a Gaussian of size 10 and standard deviation 0.5 and the subtracted background image was convolved with a Gaussian of size 20 and standard deviation 5 (LysoDoG), and thresholded (>44, LysoLocalMask). The final lysosomal mask is the overlap between CellStencilRefined, LysoGlobalMask, and LysoLocalMask (LysoMask). Sphericity was computed according to Wadell. The feret ratio is the ratio between major and minor axis length. Colocalization is defined as the proportion of mitochondrial pixels overlapping with lysosomes.

Mitochondrial ROS measurement

Mitochondrial ROS analysis was performed in an adjusted protocol (Li et al., 2011). $2*10^5$ cells per sample were grown for two days reaching 70% confluence in 24 well plate. Cells were washed once using warm HBSS, incubated with 5µM MitoSOX in HBSS for 10 min at 37°C, and washed 3x using warm HBSS. Cells were detached using 0.05% trypsin for 5 min at 37°C. Trypsin was stopped using DMEM/F12+10%FCS. Cells were fixed using 4% PFA-PBS for 20 min at RT, washed with 1xPBS and suspended in 1%FBS/PBS. Cells were directly analyzed via flow cytometer. In FSC and SSC, we first gated the NESC population; next two gates were set on SSC-A vs. SSC-H and SSC-A vs. SSC-W to exclude doublets. Based on an unstained control a MitoSOX+ gate was set as indicated. Mean fluorescence of MitoSOX+ readout was plotted.

Extracellular flux (XF) analysis

NESC were seeded in MatriGel coated XF 96-well plates (Seahorse/Agilent) in octuplicates at $6.5*10^4$ cells/well in 100 µl growth medium. The Seahorse XF Cell Mito stress test kit was used according to manufacturer's instructions (Agilent). Oligomycin, FCCP, and Rotenone/Antimycin A were used at 1 µM concentration. After the assay, cells were frozen at -80 and CyQuant kit (ThermoFisher) was used to measure DNA content for normalization. The post-normalization values of OCR and ECAR reflect both the metabolic activities of the cells and the number of cells being measured. Data were further processed using the manufacturer's calculation matrix. Briefly, the determined parameters (basal respiration level, proton leak, maximal, spare, and non-mitochondrial respiratory capacity) were calculated according to manufacturer's instructions.

Propidium iodide

$2*10^5$ NESCs per sample were grown for four days, reaching 70% confluence. Cells were dissociated using Accutase incubation for 8 min, at 37°C. After 5 min 400 rcf centrifugation, cells were washed once in 1 ml ice cold DMEM/F12 w/o phenol-red. Cells were dissociated in 300 µl DMEM/F12 w/o phenol-red and stained with a final concentration of propidium iodide of 0.33 µg/ml for 2 min at 4°C. The samples were assessed using flow cytometry.

Total ROS measurement

NESCs were plated $1.5*10^4$ in 96-well plates and grown for 4 days in maintenance condition. GSH/GSSG-Glo Assay (Promega) was performed according to the manufacturer's instructions. White flat bottom plates (Corning) were used for final readout in a Tecan Infinity 200 pro plate reader.

Mitochondrial membrane potential and content measurement

$2*10^5$ NESCs per sample were grown for four days reaching around 70% confluence. Cells were dissociated using Accutase for 8 min, at 37°C. Cells were suspended in DMEM/F-12 w/o phenol red for imaging, washed once, and stained with different solutions. A) 5 nM TMRM medium; B) 5 nM TMRM + 0.1 µM MitoTracker Green FM (MTG); C) 5 nM TMRM + 5 µM FCCP. Cells were incubated for 30 min at 37°C. MTG samples were washed once using a stain-free medium. The resulting cell suspension was analyzed by a Fortessa flow cytometry analyzer (BD Biosciences). The analysis was performed using FlowJo. In FSC and SSC, we first gated the NESC population. The next two gates were set on SSC-A vs. SSC-H and SSC-A vs. SSC-W to exclude doublets. Due to the nonparametric distribution of some samples, median fluorescence values were extracted for TMRM and MTG staining. The TMRM median MMP representing intensities were normalized to MTG values representing mitochondrial content per cell. Median MTG Mitochondrial content values were used also separately for quantification of the mitochondrial content.

Western Blotting analysis

NESC were grown at $6.25*10^4$ for 1 week. 3 wells of of a six-well plate per condition were pooled for one sample. Cells were either not treated or incubated in: chloroquine 100µM for 6h in maintenance medium, 3h or 6h chloroquine 100 µM in EBSS for additional autophagy induction. Cells were washed once using ice-cold PBS, scraped off and pelleted. Cells were lysed with lysis buffer containing: 100 mM NaCl, 20 mM Tris (pH7.0), 2 mM EDTA, 2 mM EGTA ,and supplemented with 1% Triton X-100, 0.1% SDS, 1 mM PMSF, 1 mM DTT, 50 mM NaF, 1.5 mM sodium orthovanadate and 7x protease inhibitor cocktail (Roche). The lysates were sonicated twice during approximately 5 sec each (50% amplitude) and assayed for protein content using the BioRad reagent, according to the manufacturer's instructions and stored at -80°C. Equivalent amounts of protein (70 µg) were separated from SDS-PAGE gels and electroblotted onto polyvinylidene difluoride (PVDF) membrane in CAPS/methanol 10% at 0.75 A for 2 hours. The membranes were stained with a Ponceau-S solution and washed with distilled water and 0.1 M NaOH. Two further washes were carried out with TBS, 0.1% Tween (vol/vol), for 5 min each. The membranes were blocked with 5% bovine serum albumin (BSA) in TBS 0.1% Tween (vol/vol), for 60 min at RT and incubated o/n at 4ºC with agitation with antibodies against LC3B (Cell Signaling, 1:1000, 2775), SQSTM1/p62 (Cell Signaling, 1:1000, 5114), and Beclin-1 (BD Transduction Laboratories, 1:1000, 612113). The day after, the membranes were washed three times with 1% TBS-T containing BSA and further incubated with alkaline phosphatase-conjugated secondary antibody (1:10.000) for 1 hour at RT. Proteins were visualized by using an enhanced chemifluorescent reagent (ECF) and the bands were detected with the BioRad Chemidoc Imaging System. The detected bands were analyzed using Chemidoc Imaging System (BioRad) and normalized to intensity mean of PonceauS whole protein lane. We used PonceauS for normalization because we cannot exclude effects of LRRK2-G2019S on standard housekeeping proteins.

Supplemental Reference

Foster J, Koglsberger S, Trefois C, Boyd O, Baumuratov AS, Buck L, Balling R, Antony PM. Characterization of differentiated SH-SY5Y as neuronal screening model reveals increased oxidative vulnerability. **Journal of Biomolecular Screening**. 2016;21:469-509.

Li Z, Ji G, Neugebauer V. Mitochondrial reactive oxygen species are activated by mGluR5 through IP3 and activate ERK and PKA to increase excitability of amygdala neurons and pain behavior. **Journal of Neuorscience**. 2011;31:1114-1127.

Macosko EZ, Basu A, Satija R et al. Highly Parallel Genome-wide Expression Profiling of Individual Cells Using Nanoliter Droplets. **Cell**. 2015;161:1202-1214.

Reinhardt P, Glatza M, Hemmer K et al. Derivation and expansion using only small molecules of human neural progenitors for neurodegenerative disease modeling. **PloS One**. 2013:8e59252.